J. Fluid Mech. (1994), *vol.* 274, *pp.* 219–241

Tidal excitation of hydromagnetic waves and their damping in the Earth

By R. R. KERSWELL

Department of Mathematics and Statistics, University of Newcastle upon Tyne, NE1 7RU, UK

(Received 28 April 1993 and in revised form 11 March 1994)

We examine the possibility that the Earth's outer core, as a tidally distorted fluid-filled rotating spheroid, may be the seat of an elliptical instability. The instability mechanism is described within the framework of a simple Earth-like model. The preferred forms of wave disturbance are explored and a likely growth rate supremum deduced. Estimates are made of the Ohmic and viscous decay rates of such hydromagnetic waves in the outer core. Rather than a conclusive disparity of scales, we find that typical elliptical growth rates, Ohmic decay rates and viscous decay rates all have the same order for plausible core fields and core-to-mantle conductivities. This study is all the more timely considering the recent realization that the Earth's precession may also drive similar instabilities at comparable strengths in the outer core.

1. Introduction

One of the outstanding issues in geophysics is the generation of the Earth's magnetic field. Presumed the seat of the geodynamo, the Earth's outer core has been, and remains, an area of intense interest for geophysicists and applied mathematicians alike (e.g. see the survey by Braginsky 1991, and reviews by Soward 1991, and Roberts & Soward 1992). Recent reports claiming to have identified the signatures of inertial waves in superconducting gravimetric data for the Earth (Melchior & Ducarme 1986; Aldridge & Lumb 1987; Melchior *et al.* 1988; Crossley, Hinderer & Legros 1991) have refocused interest in the normal modes of oscillation in the outer core (e.g. Smylie *et al.* 1992). Aldridge, Lumb & Henderson (1989) have proposed a simple Poincaré model for the Earth in which the outer core is approximated as an oblate spheroid containing a homogeneous incompressible fluid rotating once a day about its axis of symmetry. Although a drastic idealization, this does offer a reasonable starting point to study the oscillations of the rotationally dominated outer core.

In this paper, we outline one possible mechanism for the generation of core oscillations within the framework of the Poincaré model. The Earth suffers a tidal straining due to the gravitational tug of the Moon (and also, but less so, the Sun) which should set up an elliptical flow in the outer core (e.g. Suess 1970). Much work has addressed the instability of elliptical streamlines whether in the context of an unbounded elliptical flow (Pierrehumbert 1986; Bayly 1986; Craik 1989; Waleffe 1990), an elliptical cylinder (Gledzer *et al.* 1975; Vladimirov & Tarasov 1985; Malkus 1989; Waleffe 1989; Kerswell 1993*a*) or in an ellipsoid (Gledzer *et al.* 1974; Gledzer & Ponomarev 1977; Boubnov 1978; Roesner & Schmieg 1980; Vladimirov & Vostretsov 1986); see the review by Craik (1991) and the recent reports by Gledzer & Ponomarev (1992) and Malkus (1993). Linear theory has proved successful in explaining experimental findings. An elliptical flow fixed in space represents a

uniformly rotating flow whose rotational symmetry is disrupted by an $e^{2i\theta}$ perturbation. At small ellipticities, this distortion can be considered as periodically forcing the underlying rotating flow at twice the rotational frequency. Instability can then occur through the pairwise parametric resonance of waves whose frequencies differ by this forcing frequency (Gledzer *et al.* 1974, 1975; Vladimirov & Vostretsov 1986; Waleffe 1989). A geometry is termed resonant if two waves exist which satisfy this coupling condition. Pure subharmonic instabilities, in which the frequencies of both coupling waves are equal to the rotational frequency, form a special subclass of these resonances which have been found to be the most unstable (e.g. Waleffe 1989).

The emphasis in past work has been to establish that *some* geometries are unstable under elliptical distortion and hence only the first few hydrodynamic resonances have been identified. Here the focus is a little different. We aim to assess the probability that a *given* geometry, the Earth's outer core, may harbour an elliptical instability. This effectively reduces to addressing two questions. Is there a pair of waves close to elliptical resonance in the Earth's outer core? And if so, will their elliptical excitation overcome Ohmic and viscous dissipation? We attempt to answer the first by arguing that in any geometry there are probably two waves at, or close to, resonance. This is based upon a systematic mapping of the growth rates of the first 60 or so subharmonic instabilities against their resonant geometries. The even scatter of these resonances over geometry and the likelihood of similar spreads for other instability subsets are suggestive of a good covering of all possible geometries by resonant geometries susceptible to elliptical instability.

The answer to the second question depends crucially upon the presence of a magnetic field component to the waves, and the size of the accompanying Ohmic dissipation. In terms of the excitation rate, the effect of a magnetic field is to stabilize the instability slightly for Earth-like parameters (Kerswell 1993*a*). Only couplings between fast (period = O(day)) hydromagnetic waves were found to possess geophysically interesting growth rates and for these, Ohmic dissipation would appear to swamp any excitation (the low-frequency MAC waves studied by Hide 1966, Braginsky 1967 and Malkus 1967 are not excited to any significant level). However, a simple hydromagnetic-boundary-layer analysis reveals a much reduced Ohmic dissipation of these waves due to their small magnetic component. In fact an intriguing equipartition of Ohmic and viscous decay rates seems to emerge, which are then the same order as the elliptical excitation rate. So, rather than a conclusive separation of scales in which the elliptical instability mechanism overpowers dissipative effects or vice versa, we find instead that matters may be delicately poised.

This study is all the more timely because of the recent realization that a similar instability mechanism is operative within precessing spheroidal containers (Kerswell 1993*b*). Here the streamlines are not only elliptically distorted but sheared across each other introducing an $e^{i\theta}$ perturbation to the rotating flow. This latter effect can drive new pairwise resonances with growth rates comparable to the tidal values in an Earth precessing once every 25800 years.

The paper is organized as follows. Section 2 sketches the parametric excitation of waves in a spheroid due to the effect of an orbiting tidal body. We assume the presence of a simple toroidal magnetic field to demonstrate the possibility of hydromagnetic wave excitation. By specializing attention to the preferred subset of subharmonic resonances, we confirm explicitly the stabilizing effect of a magnetic field observed in Kerswell (1993*a*). The lowest of these resonances is none other than the well known 'middle-moment-of-inertia' instability of rotating solid bodies. Section 3 is dedicated to estimating the effect of Ohmic and viscous dissipations upon fast hydromagnetic

waves within a plausible core-like model. Here we are forced to extend our model basic magnetic field to include a poloidal component. This is crucial for a realistic estimate of the Ohmic dissipation, but, as §2 demonstrates, largely unimportant as far as the elliptical growth rate is concerned. A discussion follows in §4.

2. Tidal (elliptical) instability

We consider a rotating spheroidal container filled with an incompressible electrically conducting fluid, which carries a constant axial electric current. The tidal effect of a moon 'orbiting' the spheroid is taken to be the elliptical distortion of both velocity and magnetic fields throughout the interior which is locked into a frame rotating with the moon. Suess (1971) modelled the tidal effect as just a boundary distortion, claiming that a line vortex develops at the axis due to the nonlinear boundary layer formed.

The system is non-dimensionalized using the basic rotation rate of the fluid $\Omega = |\Omega\hat{z}|$, the mean equatorial radius of the spheroid R, the density ρ, and the magnetic permeability μ such that in the frame of the tidal body rotating at $\gamma\Omega\hat{z}$, the non-dissipative equations read

$$\frac{\mathrm{D}\boldsymbol{U}}{\mathrm{D}t} + 2\gamma\hat{\boldsymbol{z}}\times\boldsymbol{U} - \alpha^2\boldsymbol{H}\cdot\boldsymbol{\nabla}\boldsymbol{H} + \boldsymbol{\nabla}p = \boldsymbol{0}, \tag{2.1}$$

$$\frac{\mathrm{D}\boldsymbol{H}}{\mathrm{D}t} = \boldsymbol{H}\cdot\boldsymbol{\nabla}\boldsymbol{U}, \tag{2.2}$$

$$\boldsymbol{\nabla}\cdot\boldsymbol{U} = \boldsymbol{\nabla}\cdot\boldsymbol{H} = 0, \tag{2.3}$$

where the magnetic field $\boldsymbol{H}^* = \alpha\Omega R(\rho/\mu)^{1/2}\boldsymbol{H}$ and p is a modified pressure. The Alfvén number α represents the ratio of Alfvén speed to fluid rotation speed and in the core has a value of $\alpha \sim 10^{-3}$ for a 100 G toroidal field. Relative to this 'tidal frame', the elliptical basic state is

$$\boldsymbol{U}_0 = (1-\gamma)\,\boldsymbol{H}_0 = (1-\gamma)\left[-y\left(\frac{1+\beta}{1-\beta}\right)^{1/2},\quad x\left(\frac{1-\beta}{1+\beta}\right)^{1/2},\quad 0\right] \tag{2.4}$$

so that the ratio of axial current to total vorticity is α in the absence of distortion, and the boundary of the spheroid is

$$\frac{x^2}{1+\beta} + \frac{y^2}{1-\beta} + \frac{z^2}{c^2} = 1. \tag{2.5}$$

The elliptical distortion parameter β is the ratio of local strain rate to rotation rate produced by the Sun and Moon and is taken as steady at its average value of 5×10^{-8} in the outer core (see Kerswell 1993*a*). At this point, linearization about the non-axisymmetric state (2.4) leads to a set of disturbance equations in which β enters the boundary conditions. Transforming the system to the non-orthogonal elliptico-polar coordinates (s,ϕ), where

$$x = s(1+\beta)^{1/2}\cos\phi; \quad y = s(1-\beta)^{1/2}\sin\phi, \tag{2.6}$$

alleviates this problem by mapping the elliptical streamlines and field lines into circles. Bayly was the first to realize the relevance of this coordinate system to elliptical flow,

stimulating the hydrodynamic analysis of a distorted cylinder by Waleffe (1989); Vladimirov & Vostretsov (1986) used this coordinate system independently in the Russian literature. The base vectors

$$\left.\begin{aligned}\tilde{\boldsymbol{s}} &= (1+\beta)^{1/2}\cos\phi\,\hat{\boldsymbol{x}}+(1-\beta)^{1/2}\sin\phi\,\hat{\boldsymbol{y}},\\ \tilde{\boldsymbol{\phi}} &= -(1+\beta)^{1/2}\sin\phi\,\hat{\boldsymbol{x}}+(1-\beta)^{1/2}\cos\phi\,\hat{\boldsymbol{y}},\end{aligned}\right\} \tag{2.7}$$

are not orthogonal and are left unnormalized so that the 'cylindrical-polar' expressions

$$\frac{\partial\tilde{\boldsymbol{s}}}{\partial\phi}=\tilde{\boldsymbol{\phi}},\quad \frac{\partial\tilde{\boldsymbol{\phi}}}{\partial\phi}=-\tilde{\boldsymbol{s}} \tag{2.8}$$

hold. As a consequence the advective derivative and divergence operators are then identical to the familiar 'cylindrical-polar' expressions:

$$\boldsymbol{u}\cdot\boldsymbol{\nabla}=u_x\frac{\partial}{\partial x}+u_y\frac{\partial}{\partial y}+u_z\frac{\partial}{\partial z}=u\frac{\partial}{\partial s}+\frac{v}{s}\frac{\partial}{\partial\phi}+w\frac{\partial}{\partial z}, \tag{2.9}$$

$$\boldsymbol{\nabla}\cdot\boldsymbol{u}=\frac{\partial u_x}{\partial x}+\frac{\partial u_y}{\partial y}+\frac{\partial u_z}{\partial z}=\frac{1}{s}\frac{\partial(su)}{\partial s}+\frac{1}{s}\frac{\partial v}{\partial\phi}+\frac{\partial w}{\partial z}, \tag{2.10}$$

where the new velocity components u, v and w are defined as follows:

$$\boldsymbol{u}=u_x\hat{\boldsymbol{x}}+u_y\hat{\boldsymbol{y}}+u_z\hat{\boldsymbol{z}}=u\tilde{\boldsymbol{s}}+v\tilde{\boldsymbol{\phi}}+w\hat{\boldsymbol{z}}. \tag{2.11}$$

The basic state,

$$\boldsymbol{U}_0=(1-\gamma)s\tilde{\boldsymbol{\phi}},\quad \boldsymbol{H}_0=s\tilde{\boldsymbol{\phi}}, \tag{2.12}$$

now appears axisymmetric because all the azimuthal (elliptical) variation is hidden in $\tilde{\boldsymbol{\phi}}$. The complementary set of vectors

$$\tilde{\boldsymbol{l}}=\left[\frac{\cos\phi}{(1+\beta)^{1/2}},\frac{\sin\phi}{(1-\beta)^{1/2}},0\right],\quad \tilde{\boldsymbol{n}}=\left[\frac{-\sin\phi}{(1+\beta)^{1/2}},\frac{\cos\phi}{(1-\beta)^{1/2}},0\right],\quad \hat{\boldsymbol{z}}, \tag{2.13}$$

chosen so that for example $\tilde{\boldsymbol{l}}\cdot\tilde{\boldsymbol{s}}=1$, $\tilde{\boldsymbol{l}}\cdot\tilde{\boldsymbol{\phi}}=0$ and $\tilde{\boldsymbol{l}}\cdot\hat{\boldsymbol{z}}=0$, is used to project out three independent components of the momentum equation. Linearizing about the basic state (2.12), and shifting to a frame rotating with the underlying flow, the disturbance equations for perturbations in the velocity and magnetic fields $\boldsymbol{u}$ and $\boldsymbol{h}$ are exactly (in $(\tilde{\boldsymbol{s}},\tilde{\boldsymbol{\phi}},\hat{\boldsymbol{z}})$-components)

$$\begin{aligned}\frac{\partial\boldsymbol{u}}{\partial t}+2(1-\gamma+\tilde{\gamma})(-v\tilde{\boldsymbol{s}}+u\tilde{\boldsymbol{\phi}})-\alpha^2\bar{\partial}_\phi\boldsymbol{h}-2\alpha^2(-h_\phi\tilde{\boldsymbol{s}}+h_s\tilde{\boldsymbol{\phi}})+\bar{\boldsymbol{\nabla}}p\\ =\beta[\mathrm{e}^{2\mathrm{i}(\phi+[1-\gamma]t)}\mathcal{N}(\tfrac{1}{2}\bar{\boldsymbol{\nabla}}p+\mathrm{i}\tilde{\gamma}\boldsymbol{u})+\mathrm{e}^{-2\mathrm{i}(\phi+[1-\gamma]t)}\mathcal{N}^*(\tfrac{1}{2}\bar{\boldsymbol{\nabla}}p-\mathrm{i}\tilde{\gamma}\boldsymbol{u})],\end{aligned} \tag{2.14}$$

$$\frac{\partial\boldsymbol{h}}{\partial t}-\bar{\partial}_\phi\boldsymbol{u}=\boldsymbol{0}, \tag{2.15}$$

and

$$\boldsymbol{\nabla}\cdot\boldsymbol{u}=\boldsymbol{\nabla}\cdot\boldsymbol{h}=0, \tag{2.16}$$

where $\bar{\partial}_\phi\boldsymbol{A}=\partial_\phi\boldsymbol{A}-A_s\tilde{\boldsymbol{\phi}}+A_\phi\tilde{\boldsymbol{s}}$, i.e. $\bar{\partial}_\phi\tilde{\boldsymbol{s}}=\bar{\partial}_\phi\tilde{\boldsymbol{\phi}}=\boldsymbol{0}$,

$$\mathcal{N}=\begin{bmatrix}1 & \mathrm{i} & 0\\ \mathrm{i} & -1 & 0\\ 0 & 0 & 0\end{bmatrix},\quad \tilde{\gamma}=\frac{\gamma}{(1-\beta^2)^{1/2}},\quad \bar{\boldsymbol{\nabla}}=\tilde{\boldsymbol{s}}\frac{\partial}{\partial s}+\tilde{\boldsymbol{\phi}}\frac{1}{s}\frac{\partial}{\partial\phi}+\hat{\boldsymbol{z}}\frac{\partial}{\partial z}. \tag{2.17}$$

Here, $\bar{\nabla}$ is a pseudo-gradient operator, and the modified pressure p, axial velocity w, axial magnetic field h_z and z-coordinate have been rescaled as follows:

$$p \to (1-\beta^2)p, \quad [w, h_z, z] \to (1-\beta^2)^{1/2}[w, h_z, z].$$

The boundary condition for the velocity field remains

$$\boldsymbol{u}\cdot\hat{\boldsymbol{n}}|_{\partial V} = 0. \tag{2.18}$$

This, along with the azimuthal form of the imposed magnetic field, forces the magnetic boundary condition $\boldsymbol{h}\cdot\hat{\boldsymbol{n}}|_{\partial V} = 0$ through the induction equation: the magnetic field disturbance is confined to the spheroidal interior. Defining the 6-vector $\boldsymbol{\Psi} = [\boldsymbol{u}, \boldsymbol{h}]^T$ leads to the condensation

$$\frac{\partial \boldsymbol{\Psi}}{\partial t} - \mathscr{L}_0 \boldsymbol{\Psi} = \beta(\mathscr{L}_1^+ + \mathscr{L}_1^-)\boldsymbol{\Psi}, \tag{2.19}$$

where

$$\mathscr{L}_0 \boldsymbol{\Psi} = \begin{bmatrix} -2(-v\tilde{\boldsymbol{s}} + u\tilde{\boldsymbol{\phi}}) + \alpha^2(\bar{\partial}_\phi \boldsymbol{h} + 2[-h_\phi \tilde{\boldsymbol{s}} + h_s \tilde{\boldsymbol{\phi}}]) - \bar{\nabla} p \\ \bar{\partial}_\phi \boldsymbol{u} \end{bmatrix}, \tag{2.20}$$

$$\mathscr{L}_1^+ \boldsymbol{\Psi} = \mathrm{e}^{2\mathrm{i}(\phi + [1-\gamma]t)} \begin{bmatrix} \mathscr{N}(\tfrac{1}{2}\bar{\nabla} p + \mathrm{i}\gamma \boldsymbol{u}) \\ \boldsymbol{0} \end{bmatrix}, \tag{2.21}$$

$\mathscr{L}_1^- = (\mathscr{L}_1^+)^*$, and with quadratic and higher terms in β neglected. Of course both the left- and right-hand sides of (2.19) depend on β in terms of the base vectors $\tilde{\boldsymbol{s}}$ and $\tilde{\boldsymbol{\phi}}$ if nothing else. However, once we have transformed to (s, ϕ, z) coordinates, the components of the momentum equation along each of $\tilde{\boldsymbol{l}}$ and $\tilde{\boldsymbol{n}}$ only feel the presence of β through the right-hand-side operator. Subsequently it makes sense to expand in terms of β within this distorting system, acknowledging the fact that the β-invariant leading-order term will vary with β back in the physical (x, y, z) system. With this in mind, we consider a disturbance composed of two waves to leading order,

$$\boldsymbol{\Psi}(\boldsymbol{r}, t) = A(t)\,\boldsymbol{\Psi}_a(\boldsymbol{r}) + B(t)\,\boldsymbol{\Psi}_b(\boldsymbol{r}) + \beta\,\boldsymbol{\Theta}(\boldsymbol{r}, t) + O(\beta^2), \tag{2.22}$$

each of which solves the $\beta = 0$ version of (2.19). The time-varying amplitudes, A and B, are defined such that

$$A = \langle \boldsymbol{\Psi}_a, \boldsymbol{\Psi} \rangle \quad \text{and} \quad B = \langle \boldsymbol{\Psi}_b, \boldsymbol{\Psi} \rangle, \tag{2.23}$$

where the appropriate inner product is

$$\langle \boldsymbol{\Psi}_a, \boldsymbol{\Psi}_b \rangle = \iiint \mathrm{d}V \{(1-\alpha^2)\,\boldsymbol{Q}_a^* \cdot \boldsymbol{Q}_b + \alpha^2(\boldsymbol{Q}_a^* - \boldsymbol{H}_a^*)\cdot(\boldsymbol{Q}_b - \boldsymbol{H}_b)\} \tag{2.24}$$

as derived in Kerswell (1993*a*), and the modes are assumed normalized. Hence, in particular,

$$\langle \boldsymbol{\Psi}_a, \boldsymbol{\Theta} \rangle = \langle \boldsymbol{\Psi}_b, \boldsymbol{\Theta} \rangle = 0. \tag{2.25}$$

Equation (2.19) may be alternatively projected onto $\boldsymbol{\Psi}_a$ and $\boldsymbol{\Psi}_b$ giving the expressions

$$\frac{\partial A}{\partial t} - (\mathrm{i}\lambda_a - \nu_a) A = \beta \langle \boldsymbol{\Psi}_a, (\mathscr{L}_1^+ + \mathscr{L}_1^-)\boldsymbol{\Psi}_b \rangle B, \tag{2.26}$$

$$\frac{\partial B}{\partial t} - (\mathrm{i}\lambda_b - \nu_b) B = \beta \langle \boldsymbol{\Psi}_b, (\mathscr{L}_1^+ + \mathscr{L}_1^-)\boldsymbol{\Psi}_a \rangle A \tag{2.27}$$

to $O(\beta)$ and where we have inserted the modal decay rates to capture the leading-order effect of dissipation; these are the subject of §3.

The waves existant upon our undistorted hydromagnetic basic state, where $\beta = 0$, were first written down by Malkus (1967) who realized that they are a simple extension of the Poincaré modes for a uniformly rotating fluid (Poincaré 1885; Cartan 1922; Kudlick 1966; Greenspan 1968, p. 64). In cylindrical coordinates (r, ϕ, z), for a spheroidal container

$$r^2 + \frac{z^2}{c^2} = 1,$$

these modes take the (unnormalized) form

$$[\boldsymbol{u}(x,t), \boldsymbol{h}(x,t), p(x,t)] = [\boldsymbol{Q}(r,z), \boldsymbol{H}(r,z), \Phi(r,z)]\, \mathrm{e}^{\mathrm{i}(m\phi + \lambda t)}, \tag{2.28}$$

where

$$\Phi = r^{|m|} z^{\nu} \prod_{j=1}^{N} \left\{ \bar{x}_j^2 (\bar{x}_j^2 - 1) + \bar{x}_j^2 \left(\frac{r}{A}\right)^2 + (1 - \bar{x}_j^2) \left(\frac{z}{B}\right)^2 \right\}, \tag{2.29}$$

with

$$\boldsymbol{Q} = \frac{\lambda}{\lambda - \alpha^2 m} \begin{bmatrix} \dfrac{-\mathrm{i}}{4 - \Lambda^2} \left(\Lambda \Phi_r + \dfrac{2m}{r} \Phi \right) \\ \dfrac{1}{4 - \Lambda^2} \left(2\Phi_r + \dfrac{m\Lambda}{r} \Phi \right) \\ \dfrac{\mathrm{i}}{\Lambda} \Phi_z \end{bmatrix}, \quad \boldsymbol{H} = \frac{m}{\lambda} \boldsymbol{Q}, \tag{2.30}$$

the pseudo-frequency

$$\Lambda = \frac{\lambda^2 - \alpha^2 m^2}{\lambda - \alpha^2 m}, \tag{2.31}$$

$$A^2 = \frac{c^2 + (1 - c^2)(1 - \Lambda^2/4)}{1 - \Lambda^2/4}, \quad B^2 = \frac{c^2 + (1 - c^2)(1 - \Lambda^2/4)}{\Lambda^2/4}, \tag{2.32}$$

$$\nu = \begin{cases} 0 & \text{if} \quad n - |m| \text{ even} \\ 1 & \text{if} \quad n - |m| \text{ odd}, \end{cases} \tag{2.33}$$

and $\bar{x}_j^2$ are the $N = \frac{1}{2}(n - |m| - \nu)$ distinct squared zeros of the associated Legendre polynomial $P_n^{|m|}(\bar{x})$ in the open interval $(0, 1)$. N gives the number of zeros in r and z in a quadrant. For a given set (n, m) there are

$$k_{max} = \begin{cases} n - 1 & \text{if} \quad m = 0 \\ n - |m| & \text{if} \quad m \neq 0 \end{cases} \tag{2.34}$$

eigenfrequencies given by the no-normal-velocity boundary condition

$$\nu + 2 \sum_{1}^{N} \frac{\Lambda^2 c^2}{\Lambda^2 c^2 - \bar{x}_j^2 \{4 - \Lambda^2 (1 - c^2)\}} = \frac{m c^2 \Lambda}{2 - \Lambda} \tag{2.35}$$

for $m \geqslant 0$ (this is extendable to $m < 0$ by use of the relationship $\Lambda_{n,-m,k} = -\Lambda_{n,m,k}$). The familiar bounding of the inertial mode frequency (Greenspan 1968, p. 52) is translated to the pseudo-frequency here,

$$-2 < \Lambda < 2. \tag{2.36}$$

The matrix elements in (2.26) and (2.27) will vanish unless m_a and m_b differ by 2; to be specific we assume $m_b = m_a + 2$. These matrix elements may then be written as

$$\langle \boldsymbol{\Psi}_a, [\mathrm{e}^{-2\mathrm{i}(\phi + [1-\gamma]t)} \mathcal{N}^*(\tfrac{1}{2} \bar{\nabla} \Phi_b - \mathrm{i}\gamma \boldsymbol{Q}_b), \boldsymbol{0}]^T \rangle = C_1\, \mathrm{e}^{-2\mathrm{i}[1-\gamma]t} \tag{2.37}$$

and
$$\langle \boldsymbol{\Psi}_b, [e^{2i(\phi+[1-\gamma]t)}\mathcal{M}(\tfrac{1}{2}\bar{\nabla}\Phi_a + i\gamma Q_a), \mathbf{0}]^T\rangle = C_2 e^{2i[1-\gamma]t}, \tag{2.38}$$

where
$$C_1 = \frac{-i\pi}{2+\Lambda_a}\left\{1-2\gamma\left[1-\left(1-\frac{\alpha^2 m_b}{\lambda_b}\right)(2-\Lambda_b)\right]^{-1}\right\}J, \tag{2.39}$$

$$C_2 = \frac{i\pi}{2-\Lambda_b}\left\{1-2\gamma\left[1-\left(1-\frac{\alpha^2 m_a}{\lambda_a}\right)(2+\Lambda_a)\right]^{-1}\right\}J^*, \tag{2.40}$$

$$J = \frac{1}{(\langle \boldsymbol{\Psi}_a, \boldsymbol{\Psi}_a\rangle\langle \boldsymbol{\Psi}_b, \boldsymbol{\Psi}_b\rangle)^{1/2}}\iint r\,dr\,dz\left[\frac{\partial \Phi_a^*}{\partial r} - \frac{m_a}{r}\Phi_a^*\right]\left[\frac{\partial \Phi_b}{\partial r} + \frac{m_b}{r}\Phi_b\right], \tag{2.41}$$

and

$$\langle \boldsymbol{\Psi}, \boldsymbol{\Psi}\rangle = \frac{1-2\alpha^2 m/\lambda + \alpha^2 m^2/\lambda^2}{(1-\alpha^2 m/\lambda)^2(4-\Lambda^2)^2} \times \iiint dV\left\{\left[\Lambda\Phi_r + \frac{2m}{r}\Phi\right]^2 + \left[2\Phi_r + \frac{m\Lambda}{r}\Phi\right]^2 + \frac{(4-\Lambda^2)^2\Phi_z^2}{\Lambda^2}\right\}. \tag{2.42}$$

A further far less obvious condition is that $n_b = n_a$ otherwise J vanishes: see Appendix A of Kerswell (1993*b*) for a discussion of this requirement.

Searching for a solution of (2.26) and (2.27) in the form
$$A = A_0 e^{(\bar{\sigma}-i[1-\gamma])t}, \quad B = B_0 e^{(\bar{\sigma}+i[1-\gamma])t} \tag{2.43}$$
leads to the equations
$$[\bar{\sigma} - (1-\gamma+\lambda_a)i + \nu_a]A_0 = \beta C_1 B_0, \tag{2.44}$$
$$[\bar{\sigma} + (1-\gamma-\lambda_b)i + \nu_b]B_0 = \beta C_2 A_0, \tag{2.45}$$
and the conclusion that
$$\bar{\sigma} = \tfrac{1}{2}\{(\nu_a+\nu_b)^2 + 4\beta^2 C_1 C_2 - 4\nu_a\nu_b - (\lambda_b-\lambda_a-2[1-\gamma])^2 + 2i(\nu_a-\nu_b)(\lambda_b-\lambda_a-2[1-\gamma])\}^{1/2} + \tfrac{1}{2}[i(\lambda_a+\lambda_b) - (\nu_a+\nu_b)]. \tag{2.46}$$

At perfect tuning, $\lambda_b = \lambda_a + 2[1-\gamma]$, instability occurs when
$$\beta(C_1 C_2)^{1/2} > (\nu_a\nu_b)^{1/2}, \tag{2.47}$$
or, for no dissipation, when
$$\beta(C_1 C_2)^{1/2} > \tfrac{1}{2}(\lambda_b - \lambda_a - 2[1-\gamma]), \tag{2.48}$$
i.e. growth at resonance is exponential on a timescale of $1/\beta$ providing dissipation and detuning are sufficiently small. The above analysis is easily generalized to include additional features of the fluid flow, for example stratification (Kerswell 1993*a*; Lubow, Pringle & Kerswell 1993), by extending the dimension of the modal vector $\boldsymbol{\Psi}$ and deriving the new inner product analogous to (2.24). Additional entries may then appear in the coupling operators $\mathscr{L}_1^+$ and $\mathscr{L}_1^-$ depending crucially upon how the ellipticity enters into the underlying flow, but the overall conclusions remain the same.

To summarize, a resonance will occur between two modes $\boldsymbol{\Psi}_a$ and $\boldsymbol{\Psi}_b$ if
$$n_a = n_b, \quad m_b = m_a + 2, \tag{2.49}$$
and $\lambda_b - \lambda_a - 2[1-\gamma]$ is sufficiently small. For a given choice of k_a and k_b, the latter condition leads to a unique value of the geometry c about which there exists an $O(\beta)$ window of instability. The primary effect of the tidal orbital frequency γ is to adjust this frequency criterion and may even lead to complete stabilization. For a field-less

c	n,k	σ	c	n,k	σ
0.132620	**20 1**	**0.561826**	1.64967	18 5	0.560936
0.146932	**18 1**	**0.561671**	1.80278	3 1	0.517857
0.164703	**16 1**	**0.561455**	1.84386	7 2	0.552011
0.187356	**14 1**	**0.561142**	1.93188	20 6	0.561002
0.217218	**12 1**	**0.560663**	1.97996	16 5	0.560128
0.258363	**10 1**	**0.559875**	2.05776	12 4	0.558197
0.318627	**8 1**	**0.558436**	2.20259	8 3	0.552543
0.404174	20 2	0.561793	2.32050	18 6	0.560216
0.415140	**6 1**	**0.555348**	2.51261	14 5	0.558394
0.449413	18 2	0.561621	2.52950	4 2	0.523684
0.506302	16 2	0.561376	2.54910	9 3	0.552900
0.580138	14 2	0.561008	2.65080	20 7	0.560278
0.586436	9 1	0.559004	2.88713	10 4	0.553151
0.593004	**4 1**	**0.546530**	2.95209	16 6	0.558519
0.680103	12 2	0.560416	3.22181	5 2	0.526340
0.695914	20 3	0.561722	3.38153	18 7	0.558603
0.753134	7 1	0.556505	3.54637	12 5	0.553474
0.779850	18 3	0.561510	3.80402	20 8	0.558662
0.823770	10 2	0.559360	3.89578	6 3	0.527785
0.888292	16 3	0.561194	4.19123	14 6	0.553667
1.00000	**2 1**	**0.500000**	4.55883	7 3	0.528662
1.02600	20 4	0.561595	4.82712	16 7	0.553792
1.03451	14 3	0.560642	5.21485	8 4	0.529235
1.04995	8 2	0.557162	5.45701	18 8	0.553877
1.05827	5 1	0.549651	5.86608	9 4	0.529631
1.16509	18 4	0.561306	6.08270	20 9	0.553938
1.24477	12 3	0.559771	6.51388	10 5	0.529917
1.32188	9 2	0.557575	7.80255	12 6	0.530292
1.35308	16 4	0.560838	9.08515	14 7	0.530521
1.42203	20 5	0.561380	10.3639	16 8	0.530671
1.46646	6 2	0.551159	11.6401	18 9	0.530775
1.57749	10 3	0.557854	12.9144	20 10	0.530849
1.62430	14 4	0.559993			

TABLE 1. Growth rates of all $m = 1$ resonances (n,k) tabulated against geometry c for $n = 2, 3, 4, 5, 6, 7, 8, 9, 10, 12, 14, 16, 18, 20$. The boldfaced entries $(2n, 1)$ correspond to the dotted sequence in figure 2.

fluid, $-2 < \lambda < 2$ and hence if $\gamma > 3$ or $\gamma < -1$, no coupling can occur at $O(\beta)$ or higher orders (Craik 1989 reports such a stable interval in his unbounded analysis incorporating the Coriolis force; there his $\Omega_1 = \gamma/(1-\gamma)$). If we now specialize attention to the preferred subset of subharmonic instabilities where

$$n_a = n_b = n, \quad m_b = -m_a = 1, \quad \lambda_b = -\lambda_a = 1-\gamma \tag{2.50}$$

then, for example, the lowest subharmonic resonance, which represents a perturbation in the rotation axis of the fluid, is excited when

$$\lambda = \frac{2}{1+c^2} = 1-\gamma \Rightarrow \gamma = \frac{c^2-1}{c^2+1}. \tag{2.51}$$

For an oblate geometry, the critical γ is negative and hence the moon's motion must be retrograde to excite this mode. Condition (2.51) is none other than that the phase velocity of the mode (and its complex-conjugate partner) matches that of the moon.

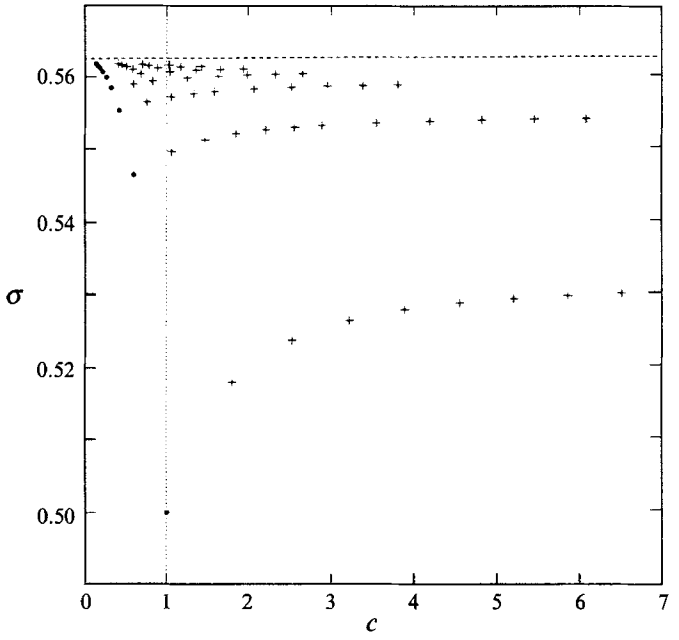

FIGURE 1. Growth rates for spinover resonances plotted against geometry c. Oblateness corresponds to $c < 1$ and prolateness to $c > 1$. A dot is used to mark the initial point on a ridge, a dashed horizontal line is drawn at $\sigma = 9/16$ and a vertical dotted line is used to mark the Earth's geometry of $c \approx 1 - 1/400$.

Other resonances between dissimilar waves represent a less successful attempt to achieve this, and their growth rates are correspondingly reduced. Note that for a sphere $\gamma = 0$, and we recover the 'middle-moment-of-inertia' instability, i.e. solid-body rotation about the intermediate principal axis is unstable ($c = 1$ is between $(1-\beta)^{1/2}$ and $(1+\beta)^{1/2}$).

Setting $\gamma = 0$, the effect of the magnetic field upon the subharmonic resonances may be isolated as being stabilizing: $m = 1$ and $\lambda = 1$ means $\Lambda = 1$ also, and allows the decoupling

$$\sigma_\alpha = (1-\alpha^2)\,\sigma, \tag{2.52}$$

where σ_α is the hydromagnetic growth rate, and σ is the $\alpha = 0$ hydrodynamic value. This special case corroborates the general conclusions of Kerswell (1993*a*).

Table 1 contains the first 60 or so subharmonic resonances when $\gamma = \alpha = 0$. Vladimirov & Vostretsov (1986) calculated the $n = 2$, 3 and 4 cases of the $m = 1$ resonances and claim good agreement with experiments. A plot of the growth rate verses c displayed in figure 1 clearly shows that both prolate and oblate spheroids can harbour elliptical instability if distorted in their equatorial plane: that is, rotation about any axis of a slightly ellipsoidal spheroid such that the streamlines are elliptical can potentially be dangerous.

The couplings are organized onto ridges which progressively asymptote to 9/16 from below, i.e. the elliptical growth rates do not drop off as the mode order increases. This figure of $9\beta/16$ appears to be a growth rate supremum for the spheroidal geometry†

† This hypothesis appears to be contradicted by some growth rate results quoted by Vladimirov & Vostretsov (1986) which surpass this supremum. However, calculations by the author confirm that these rates do in fact respect this maximum.

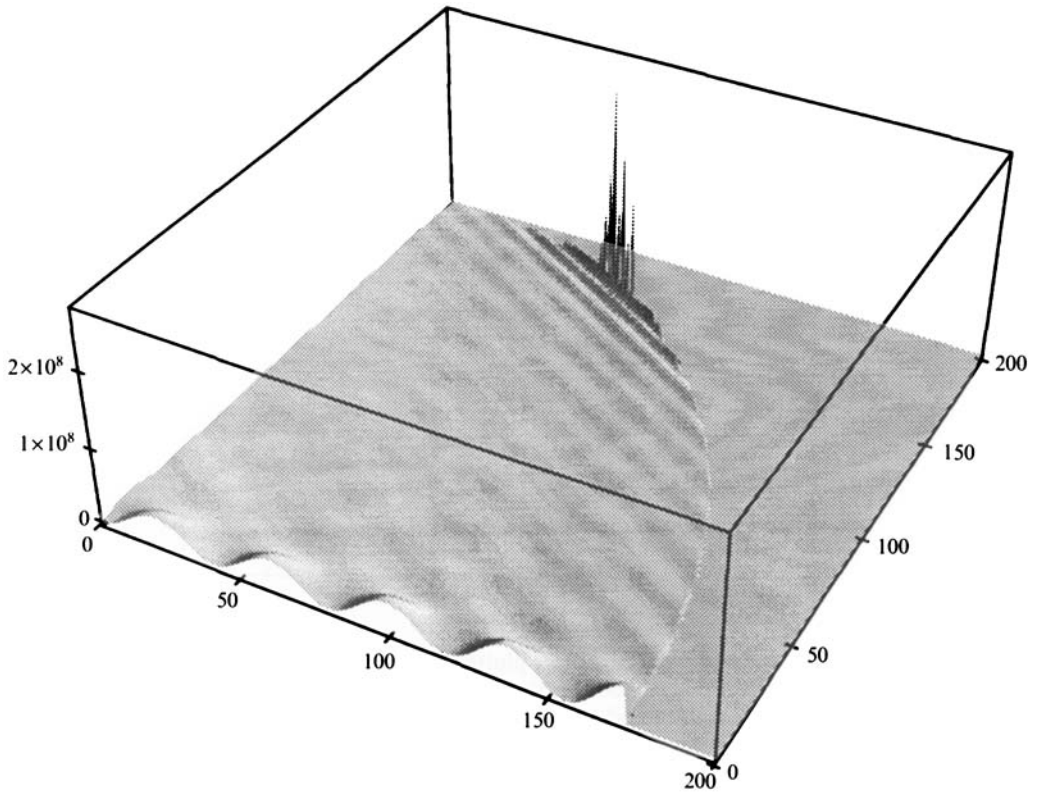

FIGURE 2. Kinetic energy density for the $\Phi_{30,1,5}$ mode. Two basic features emerge: the intense concentration of energy density at the critical latitude and the localization of energy at the rotation axis.

as it is for a cylinder (Waleffe 1989) and for plane waves in an unbounded domain (Waleffe 1990). The spheroidal subharmonic modes and their cylindrical counterparts asymptote to the same, essentially cylindrical, optimal disturbance and as a result possess a similar limiting growth rate. This is illustrated in figure 2 which plots the kinetic energy density for the $\Phi_{30,1,5}$ mode over the first quadrant of the spheroidal domain, revealing the concentration of energy at the rotation axis in the form of a string of alternating vortices. The spikes at the boundary are an inherent, but little known, feature of inertial waves which is discussed in Appendix A. Least-favoured modes in which $m = O(n)$ correspond to equatorially trapped oscillations (Wood 1981; Zhang 1993) strongly constrained by the curved boundary.

The ridges of resonances are indexed by the relative value of k to k_{max}. If $k = k_{max}$, the resonance is on the lowest branch and is the least unstable; $k_{max}-1$ ridges are higher; the $k = 1$ resonance is the most unstable for a given n. There is a countably infinite number of ridges successively layered between the highest ridge $k_{max}-9$ shown in figure 1 and the asymptote at 9/16. The resonances also become more densely concentrated upon a particular ridge as its 'degree' increases (i.e. closeness to the asymptote). Thus increasing n not only introduces further ridges but ridges with an increasing density of resonances. Around each resonance is an $O(\beta)$ danger zone which, when projected onto the geometry axis, indicates the probability of instability in a given container. This preliminary covering is further enhanced by adding ridges corresponding to other types of pairs, for example $m = 0$, 2 couplings.

To summarize, the possibility of elliptical instability is not confined to a few dangerous geometries but rather spreads across the whole spectrum of possible spheroids so that it becomes reasonable to assume that any geometry is close to a resonant geometry. At perfect tuning in the presence of dissipation, equation (2.47) indicates that instability will actually only occur if the joint elliptical growth rate exceeds the geometric mean of the individual decay rates of the wave pair. We now turn our attention to assessing the likely magnitude of these decay rates in the Earth's outer core.

3. Hydromagnetic decay rates

Owing to the Earth's rapid rotation, the lengthscales involved and the inferred diffusivities of the mainly molten iron fluid, the dissipation of wave disturbances occurs predominantly in boundary layers at the core–mantle interface and inner core surface. Gans (1971) has already explored the boundary layers associated with *slow* MAC waves in a spheroidal cavity following on from his initial work on hydromagnetic precession in a cylinder (Gans 1970). Loper (1975) considered the hydromagnetic torque produced by such layers due to the misalignment of mantle and core rotation vectors in his assessment of a precessionally driven geodynamo. Here our aim is an appraisal of these layers with a view to estimating the Ohmic and viscous decay rates of *fast* hydromagnetic waves in the outer core.

In what follows, we will not consider the inner core surface: sufficient uncertainty already exists at the core–mantle interface to make consideration of the inner core unnecessary at this stage especially as it represents only 10% of the available boundary area. We suppose that the boundary is spherical and that the conditions of no-slip apply. Magnetically, the ratio of electrical conductivities between mantle and core is the important parameter but inevitably poorly known. We concentrate upon the case of an insulating mantle but also present estimates which include mantle conductivity. Gans (1970) found that the structure of hydromagnetic boundary layers depends crucially upon whether the magnetic field permeates the boundary. As this is certainly the case in the outer core, we are forced to generalize our basic field of §2 to include a poloidal component. The presence of a toroidal field has already been found to only slightly adjust the elliptical growth rates and there is no reason to suggest that a poloidal field would behave otherwise. However, the magnetic field undoubtedly has a significant effect on the dissipation of the wave. The simplest composite field is an axisymmetric dipolar field imposed upon a uniform axial current,

$$\mathscr{H} = ar\hat{\boldsymbol{\phi}} + b\hat{\boldsymbol{z}}; \tag{3.1}$$

little is gained by considering anything more sophisticated. At this point, it is useful to redefine α^2 as 4×10^{-11}, which is the Alfvén number squared for a 1 G field. The parameters b and a then give the dipolar and toroidal field strengths in units of G; typically $b \approx 5$ and $a \approx 100$.

The magnetic component of the fast hydromagnetic waves under consideration is $O(\alpha)$ smaller than the velocity component. As a result, the viscous decay rate can be expected to assume essentially its non-magnetic value, that is $O(E^{1/2})$, where the Ekman number $E = \nu/\Omega L^2$ with $\nu = 10^{-6}\,\mathrm{m^2\,s^{-1}}$, $\Omega = 7\times10^{-5}\,\mathrm{rad\,s^{-1}}$ and $L = 3.5\times10^{6}\,\mathrm{m}$, and hence be comparable to the elliptical driving rate at $9\beta/16$. On the other hand, the Ohmic decay rate is an *a priori* unknown function of the Ohmic diffusivity measured by $E_m^{1/2}$, where the magnetic Ekman number $E_m = \eta/\Omega L^2 \approx 10^{-9}$ with $\eta = 1\,\mathrm{m^2\,s^{-1}}$, and the parameter α is the Alfvén number. The magnetic decay rate

could be $O(E_m^{1/2}) \sim 3\times10^{-5} \gg O(\beta) \sim 3\times10^{-8}$, suppressing any elliptical instability. In fact, the Ohmic decay rate will emerge to be the same order as the viscous decay rate and hence comparable with the elliptical growth rate.

The $O(1)$ frequency of fast hydromagnetic waves allows a crucial shortcut to be taken in the analysis. In this case, the Lorentz force is only an $O(\alpha^2)$ perturbation to the momentum equation (rather than $O(1)$ for slow MAC waves) which can then be decoupled from the induction equation at leading order. In the rotating frame where the fluid is at rest, the linearized equations are

$$\frac{\partial \boldsymbol{u}}{\partial t} + 2\hat{\boldsymbol{k}}\times\boldsymbol{u} + \nabla p = E\nabla^2\boldsymbol{u} + \alpha^2(\mathscr{H}\cdot\nabla\boldsymbol{h} + \boldsymbol{h}\cdot\nabla\mathscr{H}), \tag{3.2}$$

$$\frac{\partial \boldsymbol{h}}{\partial t} + \boldsymbol{u}\cdot\nabla\mathscr{H} - \mathscr{H}\cdot\nabla\boldsymbol{u} = E_m\nabla^2\boldsymbol{h}, \tag{3.3}$$

$$\nabla\cdot\boldsymbol{u} = \nabla\cdot\boldsymbol{h} = 0, \tag{3.4}$$

with $$\boldsymbol{u} = \boldsymbol{0}|_{\partial V}$$

and magnetic conditions to be discussed. We introduce the notation

$$\left.\begin{aligned} \boldsymbol{u} &= \boldsymbol{u}_0(\boldsymbol{r})\,\mathrm{e}^{st} + \tilde{\boldsymbol{u}}_0(\boldsymbol{r},t) + \epsilon[\boldsymbol{u}_1(\boldsymbol{r},t) + \tilde{\boldsymbol{u}}_1(\boldsymbol{r},t)] + \ldots,\\ \boldsymbol{h} &= \boldsymbol{h}_0(\boldsymbol{r})\,\mathrm{e}^{st} + \tilde{\boldsymbol{h}}_0(\boldsymbol{r},t) + \epsilon[\boldsymbol{h}_1(\boldsymbol{r},t) + \tilde{\boldsymbol{h}}_1(\boldsymbol{r},t)] + \ldots,\\ p &= p_0(\boldsymbol{r})\,\mathrm{e}^{st} + \tilde{p}_0(\boldsymbol{r},t) + \epsilon[p_1(\boldsymbol{r},t) + \tilde{p}_1(\boldsymbol{r},t)] + \ldots, \end{aligned}\right\} \tag{3.5}$$

and the expanded frequency

$$s = \mathrm{i}\lambda + \epsilon s_1 + \ldots, \tag{3.6}$$

with the objective of determining the real part of ϵs_1 as in Greenspan (1968, p. 56). Here a tilde refers to a boundary-layer variable and ϵ is a small expansion parameter to be determined by the boundary-layer thickness. That is, $(\boldsymbol{u}_0, \boldsymbol{h}_0, p_0)$ represents the inviscid ideal hydromagnetic wave in the interior, $(\tilde{\boldsymbol{u}}_0, \tilde{\boldsymbol{h}}_0, \tilde{p}_0)$ represents the $O(1)$ correction in the boundary layer and so forth. The hydromagnetic waves are defined by the leading-order interior problem:

$$\mathrm{i}\lambda\boldsymbol{u}_0 + 2\hat{\boldsymbol{k}}\times\boldsymbol{u}_0 + \nabla p_0 = \boldsymbol{0}, \tag{3.7}$$

$$\mathrm{i}\lambda\boldsymbol{h}_0 + \boldsymbol{u}_0\cdot\nabla\mathscr{H} - \mathscr{H}\cdot\nabla\boldsymbol{u}_0 = \boldsymbol{0}, \tag{3.8}$$

$$\nabla\cdot\boldsymbol{u}_0 = \nabla\cdot\boldsymbol{h}_0 = 0, \tag{3.9}$$

with $$\boldsymbol{u}\cdot\hat{\boldsymbol{n}} = 0|_{\partial V}.$$

No boundary condition is needed for $\boldsymbol{h}_0$ owing to the explicit form of the induction equation. The Lorentz force has been relegated to the next-order set of interior equations.

The leading-order boundary-layer system is

$$\frac{\partial \tilde{\boldsymbol{u}}_0}{\partial t} + 2\hat{\boldsymbol{k}}\times\tilde{\boldsymbol{u}}_0 - \alpha^2(\mathscr{H}\cdot\nabla\tilde{\boldsymbol{h}}_0 + \tilde{\boldsymbol{h}}_0\cdot\nabla\mathscr{H}) + \epsilon\frac{\partial\tilde{p}_1}{\partial R}\hat{\boldsymbol{R}} = E\frac{\partial^2\tilde{\boldsymbol{u}}_0}{\partial R^2}, \tag{3.10}$$

$$\frac{\partial \tilde{\boldsymbol{h}}_0}{\partial t} + \tilde{\boldsymbol{u}}_0\cdot\nabla\mathscr{H} - \mathscr{H}\cdot\nabla\tilde{\boldsymbol{u}}_0 = E_m\frac{\partial^2\tilde{\boldsymbol{h}}_0}{\partial R^2}, \tag{3.11}$$

$$\nabla\cdot\tilde{\boldsymbol{u}}_0 = \nabla\cdot\tilde{\boldsymbol{h}}_0 = 0, \tag{3.12}$$

with $$\tilde{\boldsymbol{u}}_0 + \boldsymbol{u}_0 = \boldsymbol{0}|_{\partial V}$$

using spherical polars (R, θ, ϕ). The magnetic boundary condition is that $\tilde{\boldsymbol{h}}_0 + \boldsymbol{h}_0$ fits onto an exterior potential field $\boldsymbol{h}_p$ determined uniquely by $\boldsymbol{h}_0 \cdot \hat{\boldsymbol{n}}|_{\partial V}$. The next-order problem within the interior looks like

$$\frac{\partial \boldsymbol{u}_1}{\partial t} + 2\hat{\boldsymbol{k}} \times \boldsymbol{u}_1 + \nabla p_1 = -s_1 \boldsymbol{u}_0 + \frac{\alpha^2}{\epsilon}(\mathscr{H} \cdot \nabla \boldsymbol{h}_0 + \boldsymbol{h}_0 \cdot \nabla \mathscr{H}), \tag{3.13}$$

$$\frac{\partial \boldsymbol{h}_1}{\partial t} + \boldsymbol{u}_1 \cdot \nabla \mathscr{H} - \mathscr{H} \cdot \nabla \boldsymbol{u}_1 = -s_1 \boldsymbol{h}_0, \tag{3.14}$$

with $$(\boldsymbol{u}_1 + \tilde{\boldsymbol{u}}_1) \cdot \hat{\boldsymbol{n}} = 0|_{\partial V},$$

where each perturbative effect appears to leading order. As $\nabla \cdot \tilde{\boldsymbol{u}}_0 = 0$,

$$\epsilon \frac{\partial}{\partial R}(\tilde{\boldsymbol{u}}_1 \cdot \hat{\boldsymbol{n}}) + \hat{\boldsymbol{n}} \cdot \nabla \times (\hat{\boldsymbol{n}} \times \tilde{\boldsymbol{u}}_0) = 0 \tag{3.15}$$

so $$\boldsymbol{u}_1 \cdot \hat{\boldsymbol{n}}|_{\partial V} = \frac{1}{\epsilon} \int_0^1 \mathrm{d}R\, \hat{\boldsymbol{n}} \cdot \nabla \times (\hat{\boldsymbol{n}} \times \tilde{\boldsymbol{u}}_0). \tag{3.16}$$

Note that the boundary condition for the interior magnetic field is again dictated by the induction equation, but this will turn out to be unimportant. The $O(\epsilon)$ problem in the interior is forced by the mass efflux due to the leading-order boundary-layer solution $\tilde{\boldsymbol{u}}_0$. The frequency shift s_1 is determined by a solvability condition on this problem. Formally, the appropriate hydromagnetic inner product (i.e. the modified version of (2.24) taking account of the dipolar field) is required here to suitably weight the momentum and induction equations. However, by relegating the Lorentz force to a inhomogeneous forcing at this order, the hydrodynamic inner product given by Greenspan (1968) ((2.24) with $\alpha = 0$) is sufficient for the task. In this way, the precise boundary condition on $\boldsymbol{h}_1$ is redundant: the decay rate depends solely on the mass efflux from the boundary layers. If we define

$$\langle \boldsymbol{Q}_m, \boldsymbol{Q}_n \rangle = \iiint \mathrm{d}V\, \boldsymbol{Q}_m^* \cdot \boldsymbol{Q}_n \tag{3.17}$$

and assume that all quantities have the same time dependence as the leading wave then

$$\langle \boldsymbol{u}_0, \mathrm{i}\lambda \boldsymbol{u}_1 + 2\hat{\boldsymbol{k}} \times \boldsymbol{u}_1 + \nabla p_1 \rangle + \langle \mathrm{i}\lambda \boldsymbol{u}_0 + 2\hat{\boldsymbol{k}} \times \boldsymbol{u}_0 + \nabla p_0, \boldsymbol{u}_1 \rangle$$
$$= -s_1 \langle \boldsymbol{u}_0, \boldsymbol{u}_0 \rangle + \frac{\alpha^2}{\epsilon} \langle \boldsymbol{u}_0, (\mathscr{H} \cdot \nabla \boldsymbol{h}_0 + \boldsymbol{h}_0 \cdot \nabla \mathscr{H}) \rangle. \tag{3.18}$$

This simplifies by judicious use of the divergence theorem to

$$\epsilon s_1 = \frac{-\iint \mathrm{d}S\, p_0^* \int_0^1 \mathrm{d}R\, \hat{\boldsymbol{n}} \cdot \nabla \times (\hat{\boldsymbol{n}} \times \tilde{\boldsymbol{u}}_0) + \alpha^2 \iiint \boldsymbol{u}_0^* [\mathscr{H} \cdot \nabla \boldsymbol{h}_0 + \boldsymbol{h}_0 \cdot \nabla \mathscr{H}]\, \mathrm{d}V}{\iiint |\boldsymbol{u}_0|^2\, \mathrm{d}V}, \tag{3.19}$$

which captures both the correction to the frequency due to neglecting the Lorentz force and that due to the dissipative effects. Only the first term in the numerator will contribute a real part indicating decay and it is upon this that we now concentrate.

The azimuthal structure of the hydromagnetic wave will also carry over to the boundary-layer corrections, so that

$$[\tilde{\boldsymbol{u}}_0, \tilde{\boldsymbol{h}}_0, \tilde{p}_0] = [\tilde{\boldsymbol{u}}_0(\theta), \tilde{\boldsymbol{h}}_0(\theta), \tilde{p}_0(\theta)]\, \mathrm{e}^{\mathrm{i}\lambda t + \mathrm{i}m\phi - (1-R)/\delta(\theta)}, \tag{3.20}$$

where $\delta(\theta)$ is the latitudinally dependent boundary-layer thickness. The system (3.12) becomes

$$\mathrm{i}\lambda\tilde{\boldsymbol{u}}_0 + 2\hat{\boldsymbol{k}} \times \tilde{\boldsymbol{u}}_0 - \alpha^2 \frac{\mathscr{H}_R}{\delta}\tilde{\boldsymbol{h}}_0 + \frac{\epsilon}{\delta}\tilde{p}_1 \hat{\boldsymbol{R}} = \frac{E}{\delta^2}\tilde{\boldsymbol{u}}_0, \tag{3.21}$$

$$\mathrm{i}\lambda\tilde{\boldsymbol{h}}_0 - \frac{\mathscr{H}_R}{\delta}\tilde{\boldsymbol{u}}_0 = \frac{E_m}{\delta^2}\tilde{\boldsymbol{h}}_0, \tag{3.22}$$

$$\frac{\tilde{\boldsymbol{u}}_0 \cdot \hat{\boldsymbol{R}}}{\delta} = \frac{\tilde{\boldsymbol{h}}_0 \cdot \hat{\boldsymbol{R}}}{\delta} = 0. \tag{3.23}$$

Here we have assumed

$$\frac{\mathscr{H}_R}{\delta} \gg (\mathscr{H}_\theta, \mathscr{H}_\phi), \tag{3.24}$$

so that the normal derivative dominates the tangential terms; recall that our choice (3.1) has $\mathscr{H}_R = b\cos\theta$. For this condition not to hold the poloidal field must be of $O(\delta)$ smaller than the toroidal field. For the Earth, δ_m will be found to be $\sim 10^{-5}$ and hence the criterion is sensibly satisfied over the bulk of the core–mantle boundary. At local breakdowns, where for instance $\mathscr{H}_R$ is changing sign, the layer reverts to a weaker toroidal structure. The solenoidality of both velocity and magnetic fields forces $\tilde{\boldsymbol{u}}_0 \cdot \hat{\boldsymbol{R}} = \tilde{\boldsymbol{h}}_0 \cdot \hat{\boldsymbol{R}} = 0$ throughout the layer. Eliminating $\tilde{\boldsymbol{h}}_0$ through the induction equation and taking $\hat{\boldsymbol{R}} \times$ (3.21) to remove $\tilde{p}_1$, leads to the matrix equation

$$\begin{bmatrix} -2\hat{\boldsymbol{n}}\cdot\hat{\boldsymbol{k}} & -[\mathrm{i}\lambda - \alpha^2\mathscr{H}_R^2(\mathrm{i}\lambda\delta^2 - E_m)^{-1} - E\delta^{-2}] \\ [\mathrm{i}\lambda - \alpha^2\mathscr{H}_R^2(\mathrm{i}\lambda\delta^2 - E_m)^{-1} - E\delta^{-2}] & -2\hat{\boldsymbol{n}}\cdot\hat{\boldsymbol{k}} \end{bmatrix} \begin{bmatrix} \tilde{u}_{0\theta} \\ \tilde{u}_{0\phi} \end{bmatrix} = \boldsymbol{0}. \tag{3.25}$$

For non-trivial solutions, there is the consistency relationship

$$\left(\mathrm{i}\lambda - \frac{\alpha^2\mathscr{H}_R^2}{\mathrm{i}\lambda\delta^2 - E_m} - \frac{E}{\delta^2}\right) = \pm 2\mathrm{i}\hat{\boldsymbol{n}}\cdot\hat{\boldsymbol{k}}, \tag{3.26}$$

with solutions

$$\delta^2 = \frac{-[\mathrm{i}E_m(\lambda \mp 2\hat{\boldsymbol{n}}\cdot\hat{\boldsymbol{k}}) + \alpha^2\mathscr{H}_R^2 + \mathrm{i}\lambda E] \pm \{[\mathrm{i}E_m(\lambda \mp 2\hat{\boldsymbol{n}}\cdot\hat{\boldsymbol{k}}) + \alpha^2\mathscr{H}_R^2 + \mathrm{i}\lambda E]^2 + 4EE_m\lambda(\lambda \mp 2\hat{\boldsymbol{n}}\cdot\hat{\boldsymbol{k}})\}^{1/2}}{2\lambda(\lambda \mp 2\hat{\boldsymbol{n}}\cdot\hat{\boldsymbol{k}})}, \tag{3.27}$$

where the sign option in front of the square root is independent of the others. These may be separated when $E_m \gg E$ as

$$\delta_m^2(\mp) \sim \frac{-[\mathrm{i}E_m(\lambda \mp 2\hat{\boldsymbol{n}}\cdot\hat{\boldsymbol{k}}) + \alpha^2\mathscr{H}_R^2 + \mathrm{i}\lambda E]}{\lambda(\lambda \mp 2\hat{\boldsymbol{n}}\cdot\hat{\boldsymbol{k}})} \tag{3.28}$$

and

$$\delta_v^2(\mp) \sim \frac{EE_m}{[\mathrm{i}E_m(\lambda \mp 2\hat{\boldsymbol{n}}\cdot\hat{\boldsymbol{k}}) + \alpha^2\mathscr{H}_R^2 + \mathrm{i}\lambda E]}. \tag{3.29}$$

There are four layers: two magnetic and two viscous. We define

$$\delta_m(\mp) = \delta_j \begin{cases} j=1 \\ j=2 \end{cases}; \quad \delta_v(\mp) = \delta_j \begin{cases} j=3 \\ j=4, \end{cases}$$

so that the boundary-layer variables, found as eigenvectors in (3.25), may be written

$$\tilde{\boldsymbol{u}}_0 = \sum_{j=1}^{4} a_j(\theta)[\hat{\boldsymbol{\theta}} + (-1)^{j+1}\mathrm{i}\hat{\boldsymbol{\phi}}]\,\mathrm{e}^{-(1-R)/\delta_j(\theta)+\mathrm{i}m\phi}, \tag{3.30}$$

$$\tilde{\boldsymbol{h}}_0 = \sum_{j=1}^{4} \Gamma_j(\theta)\, a_j(\theta)[\hat{\boldsymbol{\theta}} + (-1)^{j+1}\mathrm{i}\hat{\boldsymbol{\phi}}]\,\mathrm{e}^{-(1-R)/\delta_j(\theta)+\mathrm{i}m\phi}, \tag{3.31}$$

where Γ_j are defined by the induction equation as

$$\Gamma_j = \frac{\mathscr{H}_R\,\delta_j}{\mathrm{i}\lambda\delta_j^2 - E_m}. \tag{3.32}$$

The decay rate may now be expressed solely in terms of the coefficients (a_j: $j = 1,2,3,4$). Dropping the Lorentz frequency correction from (3.19), we write

$$\epsilon s_1 \langle \boldsymbol{u}_0, \boldsymbol{u}_0 \rangle = -\iint \mathrm{d}S\, p_0^* \int_0^1 \mathrm{d}R\, \hat{\boldsymbol{n}} \cdot \nabla \times (\hat{\boldsymbol{n}} \times \tilde{\boldsymbol{u}}_0) = -\int_0^{2\pi} \mathrm{d}\phi \int_0^{\pi} \mathrm{d}\theta\, p_0^* \left(\frac{\partial \bar{v}}{\partial \phi} - \frac{\partial \bar{w}}{\partial \theta} \right), \tag{3.33}$$

where

$$\bar{v} = \int_0^1 \mathrm{d}R\, \tilde{\boldsymbol{u}}_0 \cdot \hat{\boldsymbol{\phi}} = \sum_{j=1}^{4} (-1)^{j+1}\mathrm{i}a_j\,\delta_j\,\mathrm{e}^{\mathrm{i}m\phi},$$

$$\bar{w} = \int_0^1 \mathrm{d}R\, \tilde{\boldsymbol{u}}_0 \cdot \hat{\boldsymbol{k}} = \sum_{j=1}^{4} -\sin\theta a_j\,\delta_j\,\mathrm{e}^{\mathrm{i}m\phi}.$$

This formula may be rearranged through integrating by parts in θ and realizing that the boundary conditions force $\bar{w} = 0$ at $\theta = 0, \pi$. Then substituting for $\bar{v}$ and $\bar{w}$ gives expressions for the magnetic and viscous decay rates:

$$\epsilon s_1^m = \frac{\iint \mathrm{d}S \sum_1^2 a_j \delta_j \left[\dfrac{\partial p_0^*}{\partial \theta} + (-1)^{j+1} \dfrac{m p_0^*}{\sin\theta} \right]}{\langle \boldsymbol{u}_0, \boldsymbol{u}_0 \rangle}, \quad \epsilon s_1^v = \frac{\iint \mathrm{d}S \sum_3^4 a_j \delta_j \left[\dfrac{\partial p_0^*}{\partial \theta} + (-1)^{j+1} \dfrac{m p_0^*}{\sin\theta} \right]}{\langle \boldsymbol{u}_0, \boldsymbol{u}_0 \rangle}. \tag{3.34}$$

For the particular case of the lowest subharmonic mode, these expressions evaluate to

$$\mathrm{Re}\,(\epsilon s_1^m) = -E^{1/2}\frac{15}{8}\left(\frac{\alpha^2 b^2}{E_m}\right)\mathrm{Re}\int_{-1}^{1} \mathrm{d}x \frac{x^2(1+x)^2}{\left[\mathrm{i}(1-2x) + \dfrac{\alpha^2 b^2}{E_m}x^2\right]^{1/2}}, \tag{3.35}$$

$$\mathrm{Re}\,(\epsilon s_1^v) = -E^{1/2}\frac{15}{8}\,\mathrm{Re}\int_{-1}^{1} \mathrm{d}x \frac{\mathrm{i}(1+x)^2(1-2x)}{\left[\mathrm{i}(1-2x) + \dfrac{\alpha^2 b^2}{E_m}x^2\right]^{1/2}}, \tag{3.36}$$

where $x = \cos\theta$ (see Appendix B). The total decay rate $\mathrm{Re}\,(\epsilon s_1)$,

$$\mathrm{Re}\,(\epsilon s_1) = -E^{1/2}\frac{15}{8}\,\mathrm{Re}\int_{-1}^{1} \mathrm{d}x(1+x)^2\left[\mathrm{i}(1-2x) + \frac{\alpha^2 b^2}{E_m}x^2\right]^{1/2}, \tag{3.37}$$

increases monotonically as the poloidal field b grows. The most striking feature of this

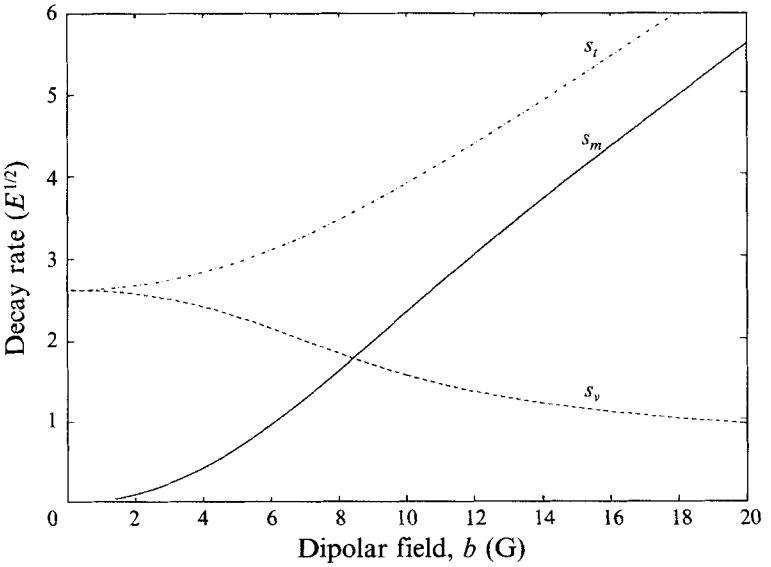

FIGURE 3. Viscous s_v and magnetic s_m decay rates for an insulating mantle. The sum s_t is also plotted to show its monotonic behaviour.

result is that the magnetic decay rate scales with $\alpha^2 b^2 E^{1/2}/E_m$. Although the exact value of the accompanying coefficient will be mode-specific, this order scaling is a generic feature determined by the small efflux velocity produced in the magnetic layer. The ratio $\alpha^2 b^2/E_m$ is typically $O(1)$ for core–mantle-boundary-like fields implying that Ohmic and viscous decay rates are of comparable magnitude; in particular,

$$\frac{\alpha^2 b^2}{E_m} = \frac{\boldsymbol{B}^2}{\Omega \mu \rho \eta} \sim 1,$$

at a dipolar field of $b \sim 5$ G. The formula (3.37) is also fairly robust, for example any potential field will give the equivalent expression

$$\mathrm{Re}\,(\epsilon s_1) = -E^{1/2}\frac{15}{8}\mathrm{Re}\int_{-1}^{1} \mathrm{d}x\,(1+x)^2\left[\mathrm{i}(1-2x)+\frac{\alpha^2}{E_m}\mathscr{H}_R^2(x)\right]^{1/2}$$

and hence have the same monotonic behaviour. Figure 3 shows how the component decay rates vary with the magnetic field strength at the boundary. The viscous layer gradually loses its strength as b increases, although any decrease in viscous dissipation is more than compensated by the increase in Ohmic dissipation. At $b = 5$ G the total decay rate is $\approx 3E^{1/2}$ compared with the elliptical growth rate of $\approx 9\beta/16 \approx 0.9E^{1/2}$; in the context of the outer core, these figures are close.

The effect of mantle conductivity can be incorporated into the above analysis relatively easily through the inclusion of an extra boundary layer in the mantle. The ratio of core-to-mantle electrical conductivities

$$\chi = \frac{\sigma_c}{\sigma_m}$$

(variously estimated as $O(1)$ to $O(10^8)$ by Li & Jeanloz 1987, 1988; Peyronneau & Poirier 1989 advocate a value of $O(10^4)$) and the high frequency of the hydromagnetic waves mean that they can only penetrate a short distance into the mantle (providing

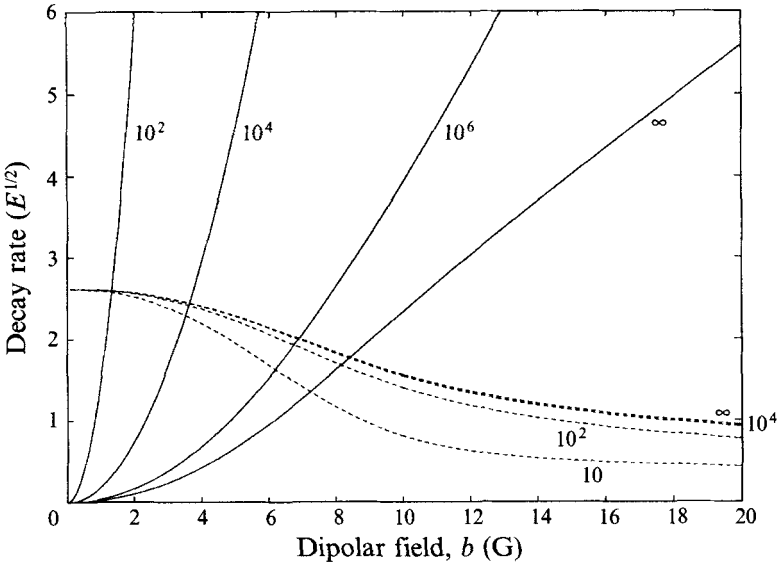

FIGURE 4. The dependence of viscous (dashed lines) and magnetic (solid lines) decay rates on χ, the ratio of core to mantle conductivity. The value of χ is used as a label, $\chi = \infty$ refers to the insulating-mantle curves. The χ = 1E6 viscous decay rate curve is not shown as it covers the insulating-mantle line.

$E_m \chi \ll 1$). Figure 4 shows how s_1^m and s_1^v vary with χ; ϵs_1^v remains $O(E^{1/2})$, but ϵs_1^m changes order. A simple scaling analysis captures the leading dependence of s_1^m on χ as

$$\epsilon s_1^m(\chi) = \begin{cases} O[\epsilon s_1^m(\infty)(E_m/E\chi)^{1/2}, & 1 \ll \chi \ll E_m/E \sim 10^6 \\ O[\epsilon s_1^m(\infty)], & E_m/E \sim 10^6 \leqslant \chi \ll 1/E_m, \end{cases} \tag{3.38}$$

where $\epsilon s_1^m(\infty)$ is the magnetic decay rate for an insulating mantle. The magnetic decay rate only differs appreciably from that for an insulating mantle when $\chi \ll E_m/E \sim 10^6$, although even at $\chi = 10^4$ there is only a tenfold increase. Specifically, a total decay rate of $3E^{1/2}$ is now achieved at a poloidal field strength of 2 G as opposed to the 5 G field needed for an insulating mantle.

4. Discussion

In this paper, we have shown how pairs of hydromagnetic waves riding upon a toroidal magnetic field may be resonantly coupled by an underlying elliptical strain. This elliptical instability is not confined to a few dangerous geometries, but appears relevant to all (distorted) spheroidal containers. The preferred form of disturbance is a column along the rotation axis of alternating coherent vortices and currents aligned with the stretching direction of the tidal straining field. The conditions for resonance are modified to maintain this alignment when the ellipticity rotates. Removal of a central segment of this columnar structure should accommodate an inner core without much disruption to the solution. Elliptical growth rates are typically $9\beta/16$ ($\sim 0.9E^{1/2}$ taking $\beta = 5 \times 10^{-8}$ and $E = 10^{-15}$), in agreement with previous results from cylindrical and unbounded domains.

The elliptical instability is simply a consequence of the $e^{2i\phi}$ perturbation to circular streamlines produced by a tidal influence. This leads to pairwise couplings between

modes whose azimuthal wavenumbers and frequencies differ by 2. A similar form of instability is driven by the Earth's precession whose dominant effect is the introduction of a $e^{i\phi}$ distortion to the streamlines at the same order as the tidal effects (Kerswell 1993*b*). This gives rise to an equally important set of pairwise 'precessional' resonances in which azimuthal wavenumbers and frequencies differ by 1.

The dissipation analysis presented above is directed at global hydromagnetic waves with periods on the daily timescale and is as pertinent to these precessional resonances as elliptical resonances. The decay rate scalings which emerge appear robust. Contrary to initial expectations, Ohmic dissipation does not necessarily swamp these resonances for Earth-like scalings by dominating viscosity (the ratio of diffusivities is a million for iron). Rather, an interesting equipartition of dissipation seems to emerge between the magnetic and viscous layers for plausible core–mantle-boundary field strengths and mantle conductivities. If χ, the ratio of core to mantle conductivity, is larger than or equal to 10^6, equipartition occurs at about $b_{equi} = 5$ G. More generally for $\chi \leqslant 10^6$,

$$b_{equi} \sim \left[\frac{EE_m \chi}{\alpha^4}\right]^{1/4},$$

where, for example, at $\chi = 10^4$, b_{equi} is still 2 G. The viscous decay rate is, and stays, $O(E^{1/2}) = O(\beta)$ as the magnetic field varies, increasing only gradually with the order of the mode; for example, there is only a factor of 4 increase from $\Phi_{2,1,1}$ to $\Phi_{30,1,5}$.

In the context of the Earth's outer core with all the uncertainties it presents, the unexpected closeness of the growth and decay rates is intriguing. We are unable to dispel tidal distortion or precession as being too weak to be important but, rather, are left to contemplate a possible balance of effects.

I am grateful to H. P. Greenspan and W. V. R. Malkus for many helpful discussions during this work.

Appendix A

The structure of inertial waves in a spheroidal container was first derived in a 'modified' oblate spheroidal coordinate system (ξ, η), defined such that

$$r = A(1-\xi^2)^{1/2}(1-\eta^2)^{1/2}, \quad z = B\xi\eta, \tag{A 1}$$

with $$A^2 = \frac{c^2+(1-c^2)(1-\Lambda^2/4)}{(1-\Lambda^2/4)}, \quad B^2 = \frac{c^2+(1-c^2)(1-\Lambda^2/4)}{\Lambda^2/4}$$

by Bryan in 1889 following the work of Poincaré (1885). In these coordinates the spheroidal domain is mapped into a rectangular region: see figure 5. The transformation is however singular when $\xi = \eta$ which occurs at the critical latitude $\Lambda = 2\hat{\boldsymbol{n}}\cdot\hat{\boldsymbol{z}}$ on the boundary: in figure 5 this is point a2 in the first quadrant and a4 in the second. Greenspan (1968, p. 191) demonstrated using a plane wave analysis that at this latitude incoming energy is reflected along the boundary instead of back into the interior. As the modal wavelength decreases, the wave 'sees' the singularity more and more, resulting in progressively more singular behaviour at this point. The critical latitude $\Lambda = 2\hat{\boldsymbol{n}}\cdot\hat{\boldsymbol{z}}$, corresponding to a latitude of

$$\tan^{-1}\frac{c^2\Lambda}{(4-\Lambda^2)^{1/2}},$$

is marked in figure 6 coinciding with the kinetic energy spike.

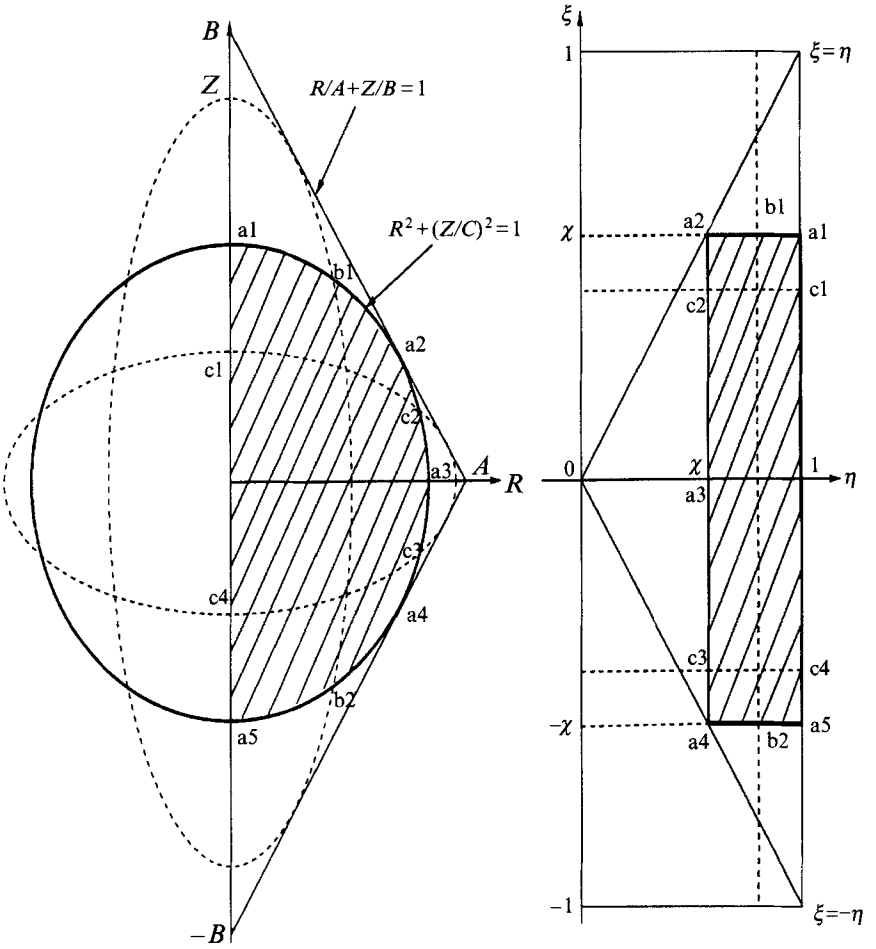

FIGURE 5. The oblate spheroidal coordinate transformation. Critical points are a2 and a4. Notation is such that, for example, elliptical arc c1–c2 in the (R, Z)-plane corresponds to the straight line c1–c2 in the (η, ξ) system.

The existence of a critical latitude for an inertial wave is well known when considering its Ekman boundary layer which has to be rescaled locally there (Roberts & Stewartson 1963). However, Wood (1977) seems to be the only previous author to appreciate that the inviscid structure of the mode also contains its signature. He considered the asymptotic structure of inertial modes with $n \gg 1$ and $m = O(1)$, finding that the velocity field takes on a cylindrical structure in which the speed is a factor $O(n^{1/2})$ larger near the rotation axis where $r = O(1/n)$ than in the interior. He also found a local $O(n)$ intensification of the velocity field at $O(1/n^2)$ distances normal to the boundary at the critical circle. These features are clearly realized in figure 2. Not unexpectedly, the critical circle plays a dominant role in the boundary-layer dissipation of these inertial modes.

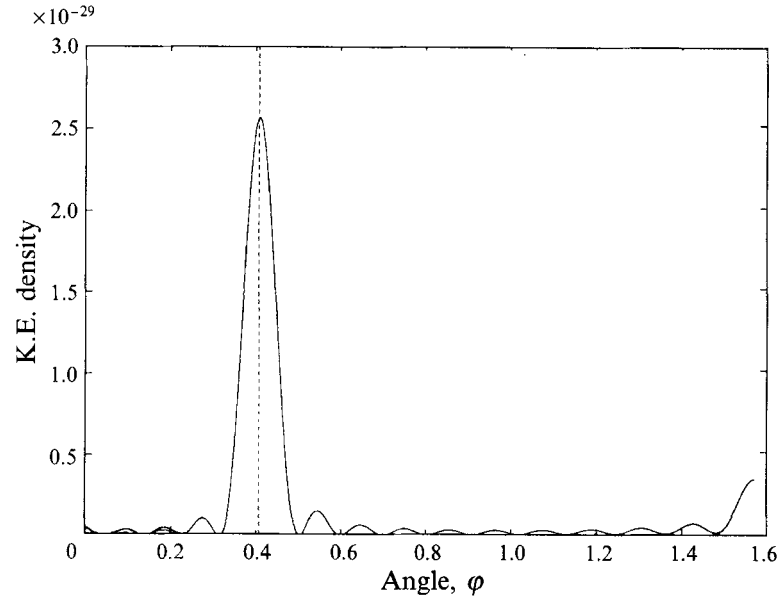

FIGURE 6. Kinetic energy density on the boundary verses latitudinal angle from the equator $z = 0$ for the $\Phi_{31,1,5}$ mode. This plot demonstrates the peaked behaviour at the critical angle $\varphi_{crit} = \tan^{-1}[(0.8644)^2/\sqrt{3}] = 0.4072$ marked by the dotted line.

Appendix B

Here we calculate the coefficient functions $a_j(\theta)$ when the leading wave solution is the lowest subharmonic mode,

$$\boldsymbol{u}_0 = \boldsymbol{Q}_{2,1,1} = \begin{bmatrix} z \\ \mathrm{i}z \\ -r \end{bmatrix}_{\hat{r},\hat{\phi},\hat{z}} \mathrm{e}^{\mathrm{i}\phi} = \begin{bmatrix} 0 \\ R \\ \mathrm{i}R\cos\theta \end{bmatrix}_{\hat{R},\hat{\theta},\hat{\phi}} \mathrm{e}^{\mathrm{i}\phi}, \tag{B 1}$$

which represents a change in the rotation axis of the fluid. This mode has a frequency $\lambda = 1$ in a spherical geometry. The induction equation prescribes the concomitant magnetic component as

$$\boldsymbol{h}_0 = \begin{bmatrix} -\mathrm{i}b\sin\theta \\ -\mathrm{i}b\cos\theta + aR \\ b + \mathrm{i}aR\cos\theta \end{bmatrix}_{\hat{R},\hat{\theta},\hat{\phi}} \mathrm{e}^{\mathrm{i}\phi}. \tag{B 2}$$

The normal component of this field at the boundary uniquely specifies the exterior potential field in the mantle as

$$\boldsymbol{h}_p = \nabla\left\{\frac{\mathrm{i}b}{2R^2}\sin\theta\,\mathrm{e}^{\mathrm{i}\phi}\right\} = \begin{bmatrix} -\mathrm{i}b\sin\theta/R^3 \\ \mathrm{i}b\cos\theta/2R^3 \\ -b/2R^3 \end{bmatrix} \mathrm{e}^{\mathrm{i}\phi}. \tag{B 3}$$

The magnetic boundary conditions then become

$$\tilde{\boldsymbol{h}}_0|_{R=1} = \begin{bmatrix} 0 \\ 3\mathrm{i}b\cos\theta/2 - a \\ -3b/2 - \mathrm{i}a\cos\theta \end{bmatrix}_{\hat{R},\hat{\theta},\hat{\phi}} \mathrm{e}^{\mathrm{i}\phi}, \tag{B 4}$$

and the full system for the coefficients a_j may now be written down:

$$a_1+a_2+a_3+a_4 = -u_{0\theta} = -1, \tag{B 5}$$

$$\mathrm{i}(a_1-a_2+a_3-a_4) = -u_{0\phi} = -\mathrm{i}\cos\theta, \tag{B 6}$$

$$\Gamma_1 a_1+\Gamma_2 a_2+\Gamma_3 a_3+\Gamma_4 a_4 = h_{p\theta}-h_{0\theta} = 3\mathrm{i}b\cos\theta/2-a, \tag{B 7}$$

$$\mathrm{i}(\Gamma_1 a_1-\Gamma_2 a_2+\Gamma_3 a_3-\Gamma_4 a_4) = h_{p\phi}-h_{0\phi} = -3b/2-\mathrm{i}a\cos\theta. \tag{B 8}$$

The relative magnitudes of the Γ indicate the degree to which the layers are coupled. Substitution of the appropriate layer thicknesses (3.28), (3.29) into the expression for Γ_j reveals that

$$\left.\begin{matrix}\Gamma_1\\ \Gamma_2\end{matrix}\right\} = \frac{\mathrm{i}(\lambda\mp 2\hat{\boldsymbol{n}}\cdot\hat{\boldsymbol{k}})}{\alpha^2\mathscr{H}_R}\left[\frac{\mathrm{i}E_m(\lambda\mp 2\hat{\boldsymbol{n}}\cdot\hat{\boldsymbol{k}})+\alpha^2\mathscr{H}_R^2+\mathrm{i}\lambda E}{-\lambda(\lambda\mp 2\hat{\boldsymbol{n}}\cdot\hat{\boldsymbol{k}})}\right]^{1/2} \sim O(E_m^{1/2}/\alpha^2 b) \sim 10^6/b \gg 1,$$

$$\left.\begin{matrix}\Gamma_3\\ \Gamma_4\end{matrix}\right\} = \frac{-\mathscr{H}_R}{E_m}\left[\frac{EE_m}{\mathrm{i}E_m(\lambda\mp 2\hat{\boldsymbol{n}}\cdot\hat{\boldsymbol{k}})+\alpha^2\mathscr{H}_R^2+\mathrm{i}\lambda E}\right]^{1/2} \sim O(bE^{1/2}/E_m) \sim O(10b). \tag{B 9}$$

Hence except for an error of $O(\alpha^2 b^2 E^{1/2}/E_m^{3/2}) \sim O(10^{-5}b^2)$, the velocity field in the viscous layer is determined by the no-slip conditions as follows:

$$a_3 = -\tfrac{1}{2}(1+\cos\theta), \quad a_4 = -\tfrac{1}{2}(1-\cos\theta). \tag{B 10}$$

Equations (B 7) and (B 8) then yield

$$a_1 = \frac{(2\Gamma_3-2\sigma+3\mathrm{i}b)(1+\cos\theta)}{4\Gamma_1}, \quad a_2 = \frac{(2\Gamma_4-2\sigma-3\mathrm{i}b)(1-\cos\theta)}{4\Gamma_2}. \tag{B 11}$$

Finally, for the mode (B 1)

$$\left[\frac{\partial p_0^*}{\partial\theta}\pm\frac{p_0^*}{\sin\theta}\right] = -\mathrm{i}(2\cos\theta\mp 1)(\cos\theta\pm 1)\mathrm{e}^{-\mathrm{i}\phi}. \tag{B 12}$$

Substitution of these results into (3.34) leads to the final expressions (3.35) and (3.36).

REFERENCES

ALDRIDGE, K. D. & LUMB, L. I. 1987 Inertial waves identified in the Earth's fluid outer core. *Nature* **325**, 421–423.

ALDRIDGE, K. D., LUMB, L. I. & HENDERSON, G. A. 1989 A Poincaré model for the Earth's fluid core. *Geophys. Astrophys. Fluid Dyn.* **48**, 5–23.

BAYLY, B. J. 1986 Three dimensional instability of elliptical flow. *Phys. Rev. Lett.* **57**, 2160–2163.

BOUBNOV, B. M. 1978 Effect of Coriolis force field on the motion of a fluid inside an ellipsoidal cavity. *Izv. Atmos. Ocean. Phys.* **14**, 151–153.

BRAGINSKY, S. I. 1967 Magnetic waves in the Earth's core. *Geomag. Aeron.* **7**, 851–859.

BRAGINSKY, S. I. 1991 Towards a realistic theory of the geodynamo. *Geophys. Astrophys. Fluid Dyn.* **60**, 89–134.

BRYAN, G. H. 1889 The waves on a rotating liquid spheroid of finite ellipticity. *Phil. Trans. R. Soc. Lond.* A **180**, 187–219.

CARTAN, M. E. 1922 Sur les petites oscillations d'une masse fluide. *Bull. Sci. Maths* **46**, 317–352.

CRAIK, A. D. D. 1989 The stability of unbounded two- and three-dimensional flows subject to body forces: some exact solutions. *J. Fluid Mech.* **198**, 275–292.

CRAIK, A. D. D. 1991 The stability of elliptical flows, unbounded and bounded. In *Proc. Intl Symp. on Generation of Large Scale Structures in Continuous Media, Moscow USSR.* (ed. R. Z. Sagdeev, U. Frisch, F. Hussain, S. S. Moiseev, N. S. Erokhin).

CROSSLEY, D. J., HINDERER, J. & LEGROS, H. 1991 On the excitation, detection and damping of core modes. *Phys. Earth Planet. Inter.* **68**, 97–116.

GANS, R. F. 1970 On hydromagnetic precession in a cylinder. *J. Fluid Mech.* **45**, 111–130.

GANS, R. F. 1971 On hydromagnetic oscillations in a rotating cavity. *J. Fluid Mech.* **50**, 449–467.

GLEDZER, E. B., DOLZHANSKIY, F. V., OBUKHOV, A. M. & PONOMAREV, V. M. 1975 An experimental and theoretical study of the stability of motion of a liquid in an elliptical cylinder. *Isv. Atmos. Ocean. Phys.* **11**, 617–622.

GLEDZER, E. B., NOVIBOV, YU. V., OBUKHOV, A. M. & CHUSOV, M. A. 1974 An investigation of the stability of liquid flows in a three-axis ellipsoid. *Isv. Atmos. Ocean. Phys.* **10**, 69–71.

GLEDZER, E. B. & PONOMAREV, V. M. 1977 Finite-dimensional approximation of the motions of an incompressible fluid in an ellipsoidal cavity. *Isv. Atmos. Ocean. Phys.* **13**, 565–569.

GLEDZER, E. B. & PONOMAREV, V. M. 1992 Instability of bounded flows with elliptical streamlines. *J. Fluid Mech.* **240**, 1–30.

GREENSPAN, H. P. 1968 *The Theory of Rotating Fluids.* Cambridge University Press.

HIDE, R. 1966 Free hydromagnetic oscillations of the Earth's core and the theory of the geomagnetic variation. *Phil. Trans. R. Soc. Lond.* A **259**, 615–647.

KERSWELL, R. R. 1993*a* Elliptical instabilities of stratified hydromagnetic waves. *Geophys. Astrophys. Fluid Dyn.* **71**, 105–143.

KERSWELL, R. R. 1993*b* The instability of precessing flow. *Geophys. Astrophys. Fluid Dyn.* **72**, 107–144.

KUDLICK, M. D. 1966 On transient motions in a contained rotating fluid. PhD thesis, MIT.

LI, X. & JEANLOZ, R. 1987 Electrical conductivity of $(Mg,Fe)SiO_3$ perovskite and a perovskite-dominated assemblage at lower mantle conditions. *Geophys. Res. Lett.* **14**, 1075–1078.

LI, X. & JEANLOZ, R. 1988 Measurement of electrical conductivity and dielectric constant of $(Mg_{0.9}Fe_{0.1})SiO_3$ perovskite. *EOS* **69**, 1436.

LOPER, D. E. 1975 Torque balance and energy budget for the precessionally driven dynamo. *Phys. Earth Planet. Inter.* **11**, 43–60.

LUBOW, S. H., PRINGLE, J. E. & KERSWELL, R. R. 1993 Tidal instability of accretion disks. *Astrophys. J.* **419**, 758–767.

MALKUS, W. V. R. 1967 Hydromagnetic planetary waves. *J. Fluid Mech.* **28**, 793–802.

MALKUS, W. V. R. 1989 An experimental study of global instabilities due to tidal (elliptical) distortion of a rotating elastic cylinder. *Geophys. Astrophys. Fluid Dyn.* **48**, 123–134.

MALKUS, W. V. R. 1993 Energy sources for planetary dynamos. In *Theory of Solar and Planetary Dynamos, NATO ASI Conf.*, Cambridge University Press.

MELCHIOR, P. W., CROSSLEY, D. J., DEHANT, V. P. & DUCARME, B. 1988 Have inertial waves been identified from the Earth's core? In *Structure and Dynamics of the Earth's Deep Interior* (ed. D. E. Smylie & R. Hide), pp. 1–12. American Geophysical Union.

MELCHIOR, P. & DUCARME, B. 1986 Detection of inertial gravity oscillations in the Earth's core with a superconducting gravimeter at Brussels. *Phys. Earth Planet. Inter.* **42**, 129.

PEYRONNEAU, J. & POIRIER, J. P. 1989 Electrical conductivity of the earth's lower mantle. *Nature* **342**, 537–539.

PIERREHUMBERT, R. T. 1986 Universal short-wave instability of 2-dimensional eddies in an inviscid fluid. *Phys. Rev. Lett.* **57**, 2157–2159.

POINCARÉ, H. 1885 Sur l'équilibre d'une masse fluide animée d'un mouvement de rotation. *Acta Mathematica* **7**, 259–380.

ROBERTS, P. H. & SOWARD, A. M. 1992 Dynamo theory. *Ann. Rev. Fluid Mech.* **24**, 459–512.

ROBERTS, P. H. & STEWARTSON, K. 1963 On the stability of a Maclaurin spheroid of small viscosity. *Astrophys. J.* **137**, 777–790.

ROESNER, K. G. & SCHMIEG, H. 1980 Instabilities of spin-up and spin-down flows inside of liquid-filled ellipsoids. *Proc. Colloqu. Pierre Curie, 1–5 Sept., Paris.*

SMYLIE, D. E., XIANHUA JIANG, BRENNAN, B. J. & KACHISHIGE SATO 1992 Numerical calculation of modes of oscillation of the Earth's core. *Geophys. J. Intl* **108**, 465–490.

SOWARD, A. M. 1991 The Earth's Dynamo. *Geophys. Astrophys. Fluid Dyn.* **62**, 191–209.

SUESS, S. T. 1970 Some effects of gravitational tides on a model Earth's core. *J. Geophys. Res.* **75**, 6650–6661.

SUESS, S. T. 1971 Viscous flow in a deformable rotating container. *J. Fluid Mech.* **45**, 189–201.

VLADIMIROV, V. A. & TARASOV, V. 1985 Resonance instability of the flows with closed stream-lines. In *Laminar-Turbulent Transition; IUTAM Symposium Novosibirsk (1984)* (ed. V. V. Kozlov), pp. 717–722. Springer.

VLADIMIROV, V. A. & VOSTRETSOV, D. 1986 Instability of steady flows with constant vorticity in vessels of elliptic cross-section. *Prikl. Matem. Mekhan.* **50(3)**, 367–377 (Transl. in *J. Appl. Math. Mech.* **50(3)**, 369–377).

WALEFFE, F. A. 1989 The 3D instability of a strained vortex and its relation to turbulence. PhD thesis, MIT.

WALEFFE, F. A. 1990 On the three-dimensional instability of a strained vortex. *Phys. Fluids* A **2**, 76–80.

WOOD, W. W. 1977 Inertial oscillations in a rigid axisymmetric container. *Proc. R. Soc. Lond.* A **358**, 17–30.

WOOD, W. W. 1981 Inertial modes with large azimuthal wavenumbers in an axisymmetric container. *J. Fluid Mech.* **105**, 427–449.

ZHANG, K. 1993 On equatorially trapped boundary inertial waves. *J. Fluid Mech.* **248**, 203–217.